World Conference on Timber Engineering Oslo 2023

GLUED-IN ROD CLT CONNECTIONS WITH FLEXIBLE POLYMER ADHESIVE

Boris Azinović[1], Václav Sebera[2], Meta Kržan[1], Andreja Pondelak[1], Jaka Gašper Pečnik[3], Arkadiusz Kwiecień[4]

ABSTRACT: This paper explores the possibility of using flexible adhesives for glued-in rods in cross laminated timber (CLT). In the first series of tests, a rod glued in a CLT panel with flexible adhesive was investigated for its mechanical resistance. The connection was tested in pull-pull configuration using monotonic and cyclic, tensile-only loading. Different glued-in lengths were tested, for which the rod diameter and glue-line thickness were constant. The tests have shown that the adhesive can resist large elastic deformations, while it does not exhibit large energy dissipation capacity. Based on the test results the numerical analyses were performed to study the behaviour of the connection where other parameters were considered. Existing constitutive models available in Ansys software were used to simulate the specific mechanical behaviour of the connection under monotonic loading. The results of the FE model exposed an optimal glue-line thickness and glued-in length in relation to the engineering design parameters. The second series of tests were material emission tests, which were carried out in a Micro-Chamber (μ-CTE) with the intention to further explore the feasibility of such connections in terms of volatile organic compound (VOC) emissions.

KEYWORDS: CLT connections, glued-in rods, flexible adhesive, polyurethane, cyclic tests, environmental aspects

1 INTRODUCTION

The glued-in rod connections are commonly used also in structures and are constructed from: i. rod, ii. adhesive and iii. structural element (e.g. structural timber, CLT etc.). In most cases such connections consist of brittle adhesive with thin bondline and a steel threaded rod. This combination of materials usually leads to a brittle failure of the connection (see e.g. [1]), where the ductile response could be reached by yielding of the rod.

In this paper, the possibility to reach a more controlled response within the adhesive layer is explored. For this purpose, a thicker bondline and a flexible polyurethane adhesive were selected for investigation. Such "flexible" glued-in rods could be used at the connection between the panel and the wall at the top and/or bottom of the wall (e.g. as hold-down connections – HD). During the seismic loading the panels are exposed to rocking, which causes the rods to be pulled out of the panels. One possible improvement by using "flexible glued-in rods" would be an increase of deformation capacity in the elastic range. Furthermore, while pulling the rod, the energy could be dissipated through the shear deformation of the adhesive layer, making the connection more ductile in comparison with brittle adhesive connections.

The prospect of building larger and taller timber buildings creates new structural design challenges due to wind and seismic actions, such as higher demands on HDs in CLT shear wall buildings: strength to resist loads, lateral stiffness to minimize deflections and damage, as well as deformation compatibility to accommodate the desired system rocking behaviour during an earthquake [2]. While in the proposal for the new Eurocode 8, the plastic deformations in HD connections are allowed [3], [4], the Canadian standard CSA 086 interprets HDs as non-dissipative connections which shall be capacity protected by designing them to remain elastic under the force and displacement demands that are induced in them when the energy-dissipative connections reach the 95th percentile of their ultimate resistance [5]. Therefore, there is also a need to develop HD solutions with high load-bearing and deformation capacities while remaining elastic. In this respect, the flexible glued-in rods could possibly meet these requirements for CLT shear walls without yielding in the (steel) rod itself.

To account for high elasticity and load-bearing capacity, recently, a hyperelastic HD solution for CLT shear walls was developed [6]. These HDs include an elastomeric bearing layer and steel plates, which were fixed inside the CLT panel by steel rods. All steel and CLT members were designed to have no inelastic deformation for a given

[1] Boris Azinović, Meta Kržan & Andreja Pondelak, Slovenian National Building and Civil Engineering Institute (ZAG Ljubljana), Slovenia, boris.azinovic@zag.si, meta.krzan@zag.si & andreja.pondelak@zag.si
[2] Václav Sebera, Mendel University in Brno (MENDELU), Czech Republic, vaclav.sebera@mendelu.cz
[3] Jaka Gašper Pečnik, InnoRenew CoE, Slovenia, jaka.pecnik@innorenew.eu
[4] Arkadiusz Kwiecień, Cracow University of Technology, Poland, akwiecie@pk.edu.pl

https://doi.org/10.52202/069179-0168

target load and therefore the HD deformations result from the rubber layers' deformation. Additionally, the overstrength factor to design the rubber layer needs to prevent the brittle failure of the CLT panel [7]. Depending on the assembly of the hyperelastic HD, the mean load bearing capacity in the study ranged from 100-150 kN, while reaching the corresponding displacements from 3-12 mm [6].

The solution presented in this paper could offer an alternative solution to the hyperelastic HD, where instead of in the rubber layer, the elastic deformation occurs in the adhesive of the glued-in rod connection. This could be achieved in a single glued-in rod connection or a combination of several glued-in rods to increase the load bearing capacity. One of the possible benefits compared to the hyperelastic HD is to retain a visible outer layer of the CLT and protect the connection in case of fire load, since it is hidden within the inner CLT layers. The paper explores the mechanical resistance of such glued-in rod connections on monotonic and cyclic axial load, while also some information on the emission tests is provided.

2 EXPERIMENTS

2.1 TENSILE RESISTANCE

The pull-pull experiments were performed on Zwick Z2500Y testing machine at the Slovenian National Building and Civil Engineering Institute (ZAG). The specimens were cut out of a 5-layer CLT (layers: 33-20-34-20-33 mm, produced according to ETA-12/0281), where the dimensions of the CLT were cca. 25 cm × 100 cm × 14 cm. For inserting the threaded rods, holes of 28 mm diameter were drilled on the tested end and 24 mm at the supported end of the CLT prisms. The rods were oriented parallel to the grain of the laminations in the middle and outer CLT layers. The test setup of the "pull-pull" test is presented in Figure 1.

At the supported end of CLT, a large diameter rod (Φ20 mm) was inserted in the 300 mm deep hole. The rod was glued to the CLT with an epoxy adhesive (HILTI RE 500) of 4 mm thickness. This ensured a large rigidity and large resistance of the fixed support. Behaviour of the rigid supporting connection was not considered in this test, since it has a negligible effect At the tested end, considered for investigation, a threaded rod with smaller diameter (Φ12 mm) was glued in the holes of 28 mm diameter (specimens' description: dh28) with an elastic polyurethane adhesive PST of 8 mm thickness, where two glued-in lengths were tested: 160 mm and 320 mm (La160 and La320). The properties of the adhesive and the timber adhesive bondline were previously determined [8]. At least three samples with the same characteristics were tested for monotonic (M) as well as for cyclic (C) tests to verify the scattering of the results. The configuration of the tested specimens is shown in Table 1.

The glued-in rods were tested under monotonic and cyclic loading in the tensile direction only. The loading was applied to the samples using a constant displacement rate of 70 mm/min. The induced displacements approximately followed the ISO 16670 displacement protocol [10]. According to ISO protocol, the small-amplitude cycles with single repetition are followed by large-amplitude cycles with three repetitions until the failure occurs. The protocol was adapted, since the connection is asymmetric, and it does not deform significantly under compression. Therefore the displacement was induced only in tension and the displacement at failure was estimated as 20 mm, what corresponds to the shear deformation angle (shear strain) of the adhesive layer equal to 250%. The real relative displacement of the connection between the rod and the CLT panel was measured with an optical extensometer which is built into the Zwick test device. The displacement was measured near the tested surface at the distance of 18 cm (Figure 1). In addition, the behaviour of the connection at the tested end was recorded with a HD camera.

Table 1: *The configuration of tests*

Specimen	α [°]	l_a [mm]	Φ_a [mm]	$\Phi_{a,r}$ [mm]	t [mm]	n
La160/M/dh28	0	160	28	12	8	4
La160/C/dh28	0	160	28	12	8	3
La320/M/dh28	0	320	28	12	8	4
La320/C/dh28	0	320	28	12	8	3

α …rod to grain angle
l_a …glued-in length
Φ_a …diameter of the hole at the tested end
$\Phi_{a,r}$ …diameter of the rod at the tested end
t …thickness of the adhesive
n …number of samples
M, C …Monotonic or Cyclic tests

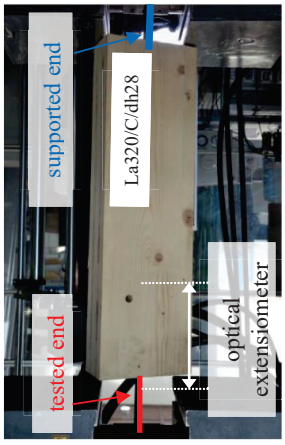

Figure 1: *Test set-up*

All deformations took place in an adhesive joint and the failure (rod pull-out) mainly occurred within the glue line (cohesive failure of the adhesive), see Figure 2. As expected, the behaviour of the connection during the monotonic loading was highly elastic, until maximum

https://doi.org/10.52202/069179-0168

load bearing capacity was reached (Figure 3). The connection resisted large deformations, while it did not prove to fail in ductile manner. The ductility values (D_f) of all tested connections were less than 1.5. The ductility value was calculated for monotonic tests as the quotient of the displacement at failure (u_f) and the displacement at the elastic load limit (u_y). The displacement u_f was determined at the 80% drop of the maximum force (F_{max}), where the displacement u_y was defined according to the method defined in EN 12512 [11].

The results (mean values with Coefficient of Variation – CoV) of monotonic loading showed elastic behaviour up to the displacement of 6.8 mm and 7.1 mm, giving ultimate shear strain of 85% and 89% (calculated for 8 mm adhesive thickness), for glued-in lengths of 160 mm and 320 mm respectively. Load-bearing capacity of the connection is approximately proportional to the glued-in length assuming all other properties are the same; mean value reaches 23.9 kN and 44.3 kN for glued-in length 160 and 320 mm respectively. Mean nominal shear strength values of the polyurethane PST adhesive (cohesive failure), calculated for the cylindrical area at the contact between the steel rod and adhesive ($\pi \times 12 \times La$) are 4.0 MPa and 3.7 MPa, respectively. Similarly, the mean stiffness values also increase by the glued-in length from 4.0 kN/mm to 6.5 kN/mm (Table 2).

Figure 2: *Rod pull-out*

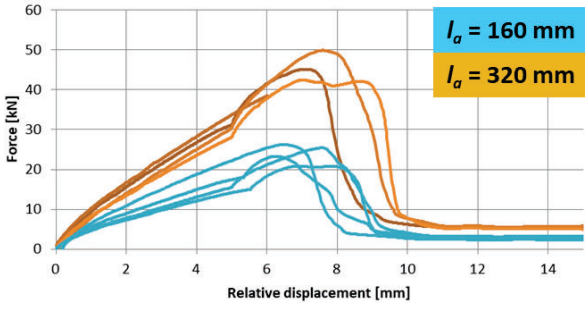

Figure 3: *Results of monotonic experiments for tested glued-in lengths 160 and 320 mm*

Table 2: *The mean results from the monotonic tests: load-bearing capacity (F_{max}), stiffness ($K_{0.1–0.4}$) and displacement at F_{max} (d_u)*

	La160/M/dh28			La320/M/dh28		
sp. no.	F_{max} [kN]	d_u [mm]	$K_{0.1–0.4}$ [kN/mm]	F_{max} [kN]	d_u [mm]	$K_{0.1–0.4}$ [kN/mm]
1	26.25	6.5	5.20	45.11	7.1	6.70
2	20.79	6.9	3.87	42.51	7.0	5.71
3	23.30	6.3	3.93	49.87	7.6	6.13
4	25.43	7.6	3.04	39.51	6.5	7.43
mn.	**23.94**	**6.8**	**4.01**	**44.25**	**7.1**	**6.49**
CoV	10.2%	8.4%	22.6%	10.0%	6.4%	11.4%

The cyclic response of the connections in terms of actuator force versus relative displacement of the joint is shown in Figure 4. The hysteretic curves for the connections with glued-in length of 160 and 320 mm showed a similar response, so only the hysteretic curves for glued-in length of 160 mm are shown, while Figure 5 shows hysteresis envelope curves for the tensile part of the cyclic test. The hysteretic curves show a typical hyperbolic strain hardening up to the maximum load capacity. This is followed by an exponential decrease in strength until failure (minimum residual load).

To characterize the performance of the connections during earthquake loading the amount of dissipated energy was evaluated in terms of equivalent viscous damping for the first cycle. The equivalent viscous damping coefficient (ξ) was evaluated from the hysteretic response as the ratio of dissipated energy (E_{DIS}) to potential energy (E_{INP}) as suggested by Chopra [12]:

$$\xi = \frac{E_{DIS}}{2\pi\, E_{INP}} \qquad (1)$$

The equivalent viscous damping coefficient was calculated for the first loading cycle and is provided in Table 3. The values for moderate amplitudes (up to the maximum load) ranged from 1% to 4.5% for glued-in length of 160 and 320 mm, respectively. The results indicate that the response is mainly elastic with little input energy dissipated.

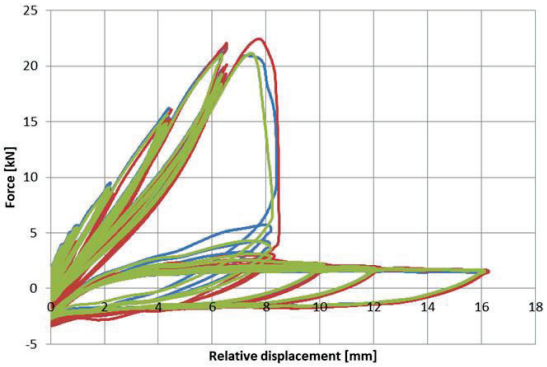

Figure 4: *Results of cyclic experiments for glued-in length 160mm*

https://doi.org/10.52202/069179-0168

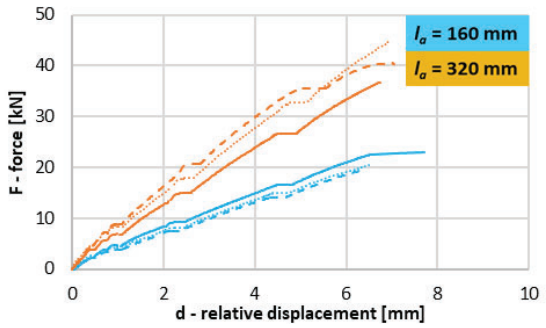

Figure 5: *Hysteresis envelopes of the cyclic tensile tests for glued-in lengths 160 and 320 mm*

Table 3: *Dissipated E_{DIS} and input energy E_{INP} of one loading cycle considered for the calculation of coefficient ξ*

	La160/C/dh28			La320/C/dh28		
sp. no.	E_{INP} [kNmm]	E_{DIS} [kNmm]	ξ [%]	E_{INP} [kNmm]	E_{DIS} [kNmm]	ξ [%]
1	33.4	2.0	0.96	113.5	29.8	4.2
2	21.4	1.3	0.94	155.0	46.4	4.8
3	22.6	1.3	0.91	140.9	35.6	4.0
mn.	**25.8**	**1.5**	**0.94**	**136.5**	**37.3**	**4.3**
CoV	25.6%	26.4%	2.7%	15.5%	22.6%	9.2%

2.2 EMISSIONS TESTS

The investigation of the connection feasibility in practise included emission tests on a CLT panel and on adhesive samples carried out in a Micro-Chamber (µ-CTE) at the Fraunhofer Institute for Wood Research WKI [13]. The purpose of the tests was to obtain general information about the emission strength of the samples and the spectrum of the emitted substances.

Sample preparation

The CLT was cut into small cubes (3 cm x 3 cm x 1 cm). The specimen contained one adhesive joint. The primer (ZP Primer) and adhesive (PS A + B) were applied in a small petri dish. The CLTs were conditioned for 15 minutes, the primer and adhesive for 30 minutes. The adhesive PS differs from the PST adhesive in terms of its mechanical response, but similarities in VOC spectra was assumed due to its source of origin.

Testing

CLT sampling was performed over 30 minutes, corresponding to a volume of about 3 litres. The primer and adhesive were tested for 10 minutes with a sampling volume of 1 litre. The difference in sampling volume was chosen because primer and adhesive are considered high emitting materials to avoid overloading the adsorbent tube. Adhesive and primer were tested in fresh – uncured state. A piece of the sample was mounted in the Micro-Chamber for emission testing (µ-CTE) in cell mode. The test was performed at 23 °C with dry synthetic air. The µ-CTE effluent was collected on a sorbent tube (Tenax TA) and analysed on a thermal desorption GC-MS system. Compounds were analysed using MS-Spectra libraries. Surface area for CLT was 27 cm^2 and the flow rate was 106.5 ml/min, while the surface area for primer and adhesive was 7 cm^2 and the flow rate was 112.8 ml/min.

Results

The Table 4 shows substances emitted from CLT, ZP Primer and adhesive PS A + B. In the case of the CLT panel, more than 30 substrates were detected with the highest concentrations of acetic acid, hexanal, formic acid, acetone, pentanal, pentanol, butanal, furaldehyde, and terpineol. Most of the substances emitted from CLT panels (organic acids, aldehydes and terpenoids) are substances characteristic of wood-based materials [14]. The highest concentrations emitted from the primer were 1-Methoxy-2-propyl acetate, Ethylbenzene and Xylene and formylmorpholine and Xylene in the case of adhesive (Table 4).

The µ-CTE emission tests were performed to obtain general information about the emitted substances from the CLT panel, the flexible adhesive, and the primer. The CLT emitted organic acids, aldehydes and terpenes, which are characteristic of wood-based materials. The primer (ZP) released a range of solvents, with 1-methoxy-2-propyl- acetate, xylene- isomers and C3-benzenes being the most abundant substances. Emissions from adhesive (PS A +B) were much lower, with N-formylmorpholine being released at higher concentrations. As mentioned above, the aim was to assess which volatile compounds were emitted by selected materials. The measurements were made on small samples (27 cm^2 or 7 cm^2) with different sampling volumes (one or three litres) and different result delivery (µg/h*m^2 or µg/h*g), so the measurements cannot be compared with each other.

3 NUMERICAL ANALYSIS

The numerical simulations using the finite element method consisted of three different analyses with the objectives: 1) to study whether it is possible to model a threaded rod without threads; 2) to simulate the real size problem and validate it through conducted experiments; and 3) to perform parametric studies for different glued-in lengths and adhesive thicknesses.

The finite element package Ansys [15] was used for all analyses. All solids were modelled using SOLID185 finite elements. All models were symmetrical, so only a quarter of the problem was modelled to reduce computational effort. Wood was modelled as a linear orthotropic material with the following properties: E_L = 14850, E_R = 352, E_T = 289, E_{LR} = 573, E_{RT} = 53, E_{LT} = 474 [MPa], μ_{LR} = 0.023, μ_{RT} = 0.557, μ_{LT} = 0.014 [-], where L, R, and T stand for longitudinal, radial and tangential anatomical directions, respectively. Steel rod was modelled as linear isotropic material with E = 200 GPa and µ = 0.3. The PST adhesive was modelled as hyperelastic material with Yeoh 3 parametric model given as c_{10} = 1.6641, c_{20} = -0.49288, c_{30} = 0.14807, $d_{1,2,3}$ = 0 that was curve-fitted to following experimental stress/strain data: 0/0.0173, 0.1/0.933, 0.2/1.541, 0.3/2.025, 0.4/2.392, 0.5/2.645, 0.6/2.838, 0.7/3.001 [MPa/-].

https://doi.org/10.52202/069179-0168

Table 4: *Results of the chamber emission test of CLT panel, ZP Primer and adhesive PS A + B*

CLT panel		**ZP Primer**		**PS A + B**	
Substance	**SER_A / µg/h*m²** (V=3L)	**Substance**	**SER_m / µg/h*g** (V=1L)	**Substance**	**SER_m / µg/h*g** (V=1L)
acetone	130	acetone	0.059	2-Butanone (MEK)	0.079
2-propanol	24	2-Butanone (MEK)	0.088	Acetic acid	0.482
Formic acid	159	Acetic acid	0.324	Toluene	0.037
Butanal	28	Toluene	0.088	2,4-Pentanedione	0.226
2-Butanone (MEK)	9	Phenol	<0.029	n-Hexanal	0.037
Acetic acid	2468	Carbon disulfide	0.029	n-Buthyl acetate	0.11
n-Butanol	12	Ethylbenzene	8.386	1-(2-Propenyloxy)-2-propanol	0.045
Propanoic acid	7	1-Methoxy-2-propyl acetate	57.705	Ethylbenzene	0.684
Pentanal	85	m,p-Xylene	23.865	1-Methoxy-2-propyl acetate	7.298
Toluene	2	2-Methoxy-1propyl acetate	0.235	m,p-Xylene	3.151
n-Pentanol	47	o-Xylene	15.537	o-Xylene	1.166
n-Hexanal	282	C9 (nonane)	0.056	n-Heptanal	0.037
2-Furaldehyde	57	Glykolester	0.088	Ethoxypropyl acetate	0.305
2-Heptanone	2	Methylstyren	0.235	Phenol	0.037
n-Heptanal	2	Propylene glycol diacetate	0.118	Octanal	0.037
Alpha-Pinene	57	p-Cymene	0.088	Methylstyren	0.605
Camphene	5	Indane	4.323	1,4-Diazabicyclo[2.2.2]octane (DABCO)	0.666
trans-2-Heptenal	5	Dimethystyren	0.177	n-Nonanal	0.098
Benzaldehyde	5	Naphtalene	<0.029	N-Formylmorpholine	18.236
Hexanoic acid	7	1-Dodecanol	0.029	n-Decanal	0.067
Phenol	2	Sum of C3 benzenes	69.916		
Beta-Pinene	14				
2,2,4,6,6-Pentamethylheptane	5				
Octanal	2				
3-Carene	5				
Limonele	9				
trans-2-Octenal	5				
n-Nonanal	5				
alpha-Terpineol	33				
C14 /tetradecane)	2				
Longifolene	9				
Carbon disulfide	7				

SER_A = Surface area-specific emission rate; SER_m = mass-specific emission rate

https://doi.org/10.52202/069179-0168

Boundary conditions (BC) consisted of: 1) fixing two sides of the block against movement; 2) symmetrical BC's were applied on two other sides; 3) pulling the rod in its axis by 6 mm in a monotonic way. At each step of the rod displacement, the force was read to generate force-displacement diagrams.

3.1 THREADING ANALYSIS

To determine if threading is important to be included in the analysis, the analysis was performed with and without threading. The model (Figure 6) was reduced to a length of 11 mm to reduce computational complexity, and a sensitivity study of mesh density was also performed.

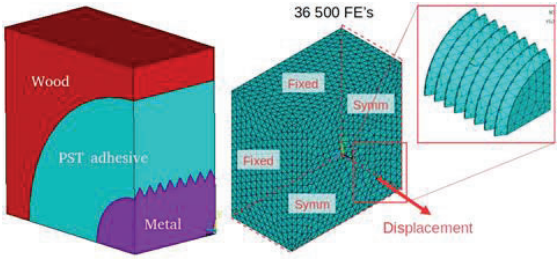

Figure 6: *Symmetrical geometry (left) and FE mesh and BC's (right) of model for thread analysis*

The model resulted in three data series as a function of mesh density (Figure 7). It is clear that the model with M11 thread (red line) behaves according to the same pattern as the models without thread with 10 and 12 mm diameter, and it is between them. This is an important finding because we can omit the thread in the full-scale models without losing the correct overall force-deflection response.

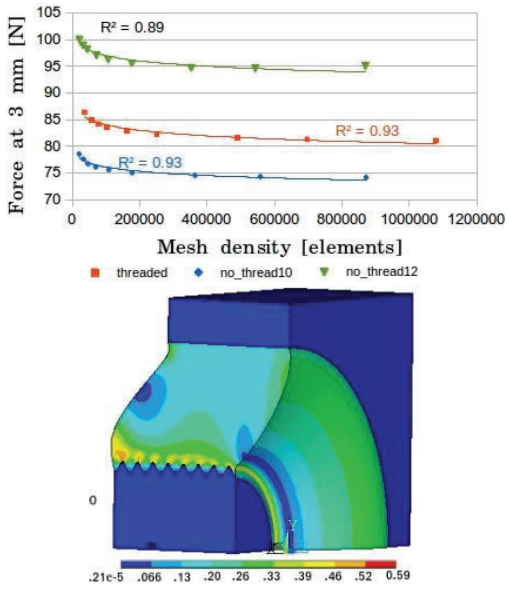

Figure 7: *Threaded vs. non-threaded models depending on mesh density (left) and von Mises Strain around threading*

Figure 7 (right) also shows that the highest strain occurs at the tips of the threads, which could indicate the position of failure initiation.

3.2 VALIDATION WITH EXPERIMENTS

A full-size 3D FE model was made in two lengths reflecting the physical experiments. The comparison of the FE models (blue and red lines) with the experiments (grey and black lines) is shown in Figure 8. The FE models of both lengths predict well the behaviour found in the experiments in terms of stiffness and hyperelastic progression of the force versus displacement. The FE models predict the behaviour up to a displacement of 6 mm, not taking into account the strength limit of the PST adhesive.

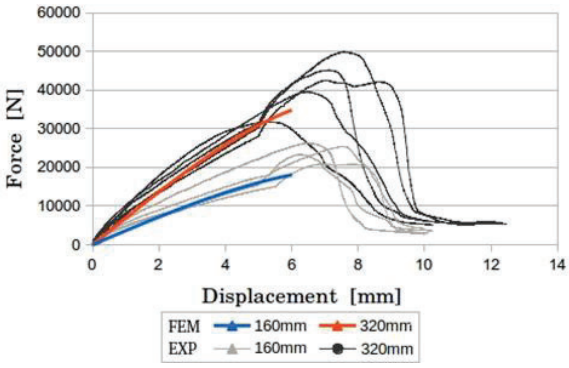

Figure 8: *Comparison of FE models (blue and red line) with experiments (grey and black lines) for both rod lengths*

3.3 PARAMETRIC STUDY

The parametric studies investigated the influence of the glued-in rod length and bondline thickness (Figure 9).

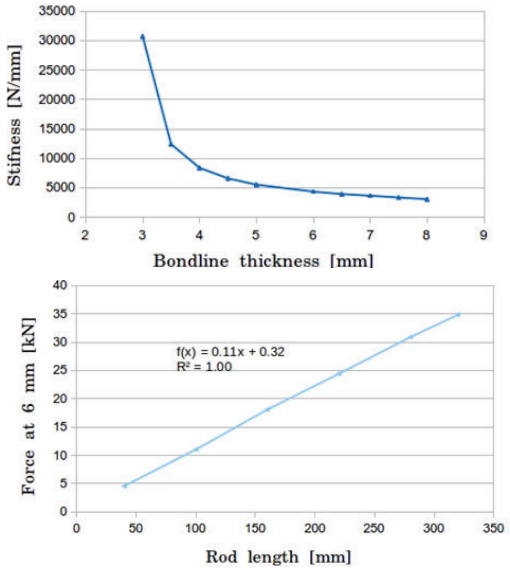

Figure 9: *Influence of bondline thickness on stiffness (top) and influence of glued-in rod length on force (bottom)*

https://doi.org/10.52202/069179-0168

These studies were performed on a full-size model (quarter-symmetrical) and did not include threads. The effect of rod length on force shows a linear trend. The effect of bondline thickness on connection stiffness, on the other hand, shows a hyperbolic trend with a decreasing tendency. Both parametric studies allow the glued-in rod connection with the CLT panel to be designed as required for the given conditions - for specific structural design. Future FE studies should focus on extending the hyperelasticity to include the range of plastic strains, so that the failure of the bonded PST connection can also be predicted, as this is the predominant failure observed in experiments.

4 CONCLUSIONS

Monotonic and cyclic tensile tests were performed on rods bonded with a flexible adhesive in CLT. The tests showed promising behaviour of such connections in terms of their elastic deformability under cyclic loading. On the other hand, a rather brittle failure with limited ductility occurred. Also, the energy dissipation capacity at larger amplitudes was not significant. The tests have also shown that the load-bearing resistance of the connection is proportional to the rod length.

To test the behaviour of the "flexible" glued-in rods when applied in CLT buildings, a series of numerical analyses were performed. First, the numerical model of the connection was calibrated based on the experimental results. The material model was able to simulate the linear part (stiffness) of the connection and provided a relatively good agreement with the experimental results. In the next phase, the model of the connection was used for the parametric study of the glued-in length and bondline thickness. The results showed that the effect of the rod length on the force exhibited a linear trend, while the bondline thickness showed a hyperbolic trend on connection stiffness with decreasing pattern. Both parametric studies demonstrate that the glued-in rod connections in CLT panels can be designed to meet the required boundary conditions in CLT walls.

Additionally, the Micro-Chamber emission tests were carried out in order to obtain general information about the emitted substances from the CLT panel, flexible adhesive and primer. The CLT panel showed the release of organic acids, aldehydes and terpenes characteristic for wood-based materials. The Primer (ZP) released a range of solvents with 1-methoxy-2-propyl-acetate, xylene-isomers and C3-benzenes as most abundant substances. Emissions of adhesive (PS A +B) were much lower with emission of N-formylmorpholine in higher concentrations.

The results of the study show a potential of using CLT wall system with “flexible” glued-in rods in seismic areas. However, future studies are necessary to investigate the long-term behaviour and performance of such connections at elevated temperatures. Also, an improvement of the performance in the nonlinear part of the connection would be essential for its actual applications.

ACKNOWLEDGEMENTS

The authors gratefully acknowledge the European Cooperation in Science and Technology for funding the InnoRenew CoE project [grant agreement #739574] under the H2020 Spreading Excellence and Widening Participation Horizon2020 Widespread-Teaming program, and Slovenian research programs P2-0273 and P4-0430; Javna Agencija za Raziskovalno Dejavnost RS. The financial support by the National Science Centre, Poland under the OPUS call in the Weave programme, No. 2021/43/I/ST8/00554 is also gratefully acknowledged.

REFERENCES

[1] B. Azinović, E. Serrano, M. Kramar, and T. Pazlar. Experimental investigation of the axial strength of glued-in rods in cross laminated timber. *Mater. and Struct*., 51(6), 2018.

[2] T. Tannert and C. Loss. Contemporary and Novel Hold-Down Solutions for Mass Timber Shear Walls. *Buildings*. 12(2):202, 2022.

[3] M. Follesa et al. The new provisions for the seismic design of timber buildings in Europe. *Eng. Struct.*, 168:736–747, 2018.

[4] M. Follesa et al. A proposal for a new Background Document of Chapter 8 of Eurocode 8. In: *INTER,* Šibenik, Croatia, 2015.

[5] CSA Standard O86-09 Engineering design in wood, Mississauga, Ontario, Canada, 2009.

[6] H. Asgari, T. Tannert, M. M. Ebadi, C. Loss, and M. Popovski. Hyperelastic hold-down solution for CLT shear walls. *Constr. Build. Mater.*, 289:123173, 2021.

[7] H. Asgari, T. Tannert, and C. Loss. Block tear-out resistance of CLT panels with single large-diameter connectors. *Eur. J. Wood Prod*., 80(4):805–816, 2022.

[8] J. G. Pečnik et al. Mechanical performance of timber connections made of thick flexible polyurethane adhesives. *Eng. Struct*., 257:113125, 2021.

[9] ISO 21581:2010 Timber structures - Static and cyclic lateral load test methods for shear walls.

[10] ISO 16670:2003 Timber structures - Joints made with mechanical fasteners - Quasi-static reversed-cyclic test method.

[11] EN 12512:2005 Timber structures - Test methods - Cyclic testing of joints made with mechanical fasteners. *Brussels:* CEN, 2005.

[12] Chopra A. K.: Dynamics of structures, 3rd Edition. Pearson Prentice Hall Hoboken, 2006.

[13] Schieweck A.: Test report No. MAIC-2019-4014: Emission test of a CLT panel and an adhesive sample. Fraunhofer WKI, Braunschweig, 2019.

[14] G. Kain et al. Qualitative investigation on VOC-emissions from spruce (Picea abies) and larch (Larix decidua) loose bark and bark panels. *Eur. J. Wood Prod.* 78(2): 403–412, 2020.

[15] ANSYS R19.2. *Ansys Inc, USA*, 2019.

https://doi.org/10.52202/069179-0168